Article

Implications of Hf isotopes for the evolution of the mantle source of magmas associated with the giant El Teniente Cu-Mo megabreccia deposit, central Chile

Charles R. Stern[1,*], Kwan-Nang Pang[2], Hao-Yang Lee[2], M. Alexandra Skewes[1], Alejandra Arévalo[3]

[1] Department of Geological Sciences, University of Colorado, Boulder, Colorado, 80309-0399 USA; Charles.Stern@colorado.edu
[2] Institute of Earth Sciences, Academia Sinica, Taipei, Taiwan; knpang@earth.sinica.edu.tw
[3] Escuela de Ingeniería, Universidad de O´Higgins, VI Región, Chile; aarevalot@gmail.com
* Correspondence: Charles.Stern@colorado.edu; Tel. +1-303-492-7170

Abstract: We have determined Hf isotopic compositions of 12 samples associated with the giant El Teniente Cu-Mo deposit, Chile. The samples range in age from ≥8.9 to 2.3 Ma and provide information about the temporal evolution of their magmatic sources from the Late Miocene to Pliocene. Together with previously published data, the new analysis indicate a temporal decrease of 10 $\varepsilon_{Hf(t)}$ units, from +11.6 down to +1.6, in the 12.7 m.y. from 15 to 2.3 Ma. These variations imply increasing incorporation of continental crust through time in the magmas that formed these rocks. The fact that the samples include mantle-derived olivine basalts and olivine lamprophyres suggests that these continental components were incorporated into their mantle source, and not by intra-crustal contamination (MASH). We attribute the increase, between the Middle Miocene and Pliocene, of crustal components in the subarc mantle source below El Teniente to be due to increased subduction erosion and transport of crust into the mantle. The deposit formed above a large, long-lived, vertically zoned magma chamber that developed due to compressive deformation and persisted between the period ~7 to 4.6 Ma. Progressively more hydrous mantle-derived mafic magmas feed this chamber from below, providing heat, H_2O, S and metals, but no unique "fertile" Cu-rich magma was involved in the formation of the deposit. As the volume of these mantle-derived magmas decreased from the Late Miocene into the Pliocene, the chamber crystallized and solidified, producing felsic plutons and large metal-rich magmatic-hydrothermal breccias that emplaced Cu and S into the older (≥8.9 Ma) mafic host rocks of this megabreccia deposit.

Keywords: El Teniente Cu-Mo deposit, Andean magmatism, subduction erosion, mantle source region contamination, Hafnium isotopes

1. Introduction

The isotopic compositions ($^{87}Sr/^{86}Sr$ ≥0.7050; ε_{Nd}≤-2; ε_{Hf}≤+2) of some recently erupted Andean volcanic rocks indicate that they have incorporated continental crust. Two very different processes for the incorporation of crust into Andean magmas have been proposed (Figure 1) [1]. One, MASH (Mixing, Assimilation, Storage and Homogenization) involves intra-crustal assimilation of crust as mantle-derived magmas rise from their source through the crust to the surface [2]. Another (PEELED) involves mantle source region contamination by crustal components subducted below the mantle wedge and released into the wedge by either melting or dehydration and volatile transport [3,4]. These two different models have very different implications for geochemical cycling associated with subduction zones, and for the growth and evolution of both the continental crust and mantle [5].

Preprints (www.preprints.org) | NOT PEER-REVIEWED | Posted: 29 July 2019 doi:10.20944/preprints201907.0327.v1

The amount of crustal components incorporated into recently erupted Andean volcanic rocks varies along strike from south-to-north, as do various geologic and tectonic features such as crustal thickness and age, subduction angle, trench depth and sediment fill, and the localized presence of bouyant features such as oceanic seamount chains and spreading ridges being subducted below the South American continental margin (Figure 2) [4]. For instance, in the Central Volcanic Zone (CVZ) of northern Chile, the crust is much thicker (≥70 km) than below the central part of the Southern Volcanic Zone (≤35 km; CSVZ; Figure 2) and the isotopic compositions of the recently erupted volcanic rocks suggests more crustal components have been incorporated in CVZ than CSVZ magmas [3-5]. This could reflect greater amounts of crustal assimilation by mantle-derived magmas as they rose through the thicker CVZ crust, but in this same region the trench is devoid of sediment due to the arid conditions in northern Chile, and compared to the CSVZ, much more significant amounts of subduction erosion, at rates estimated to be 50–70 km^3/km/my since ~150 Ma (Figure 2) [5], have truncated the continental margin [6] and caused the arc to migrate eastward ~250 km since the Jurassic (Figure 1). The subduction of tectonically eroded crust has been invoked not only to explain the crustal components in CVZ magmas [3-5,7,8], but also the uplift and crustal thickening observed in this part of the Andes [9].

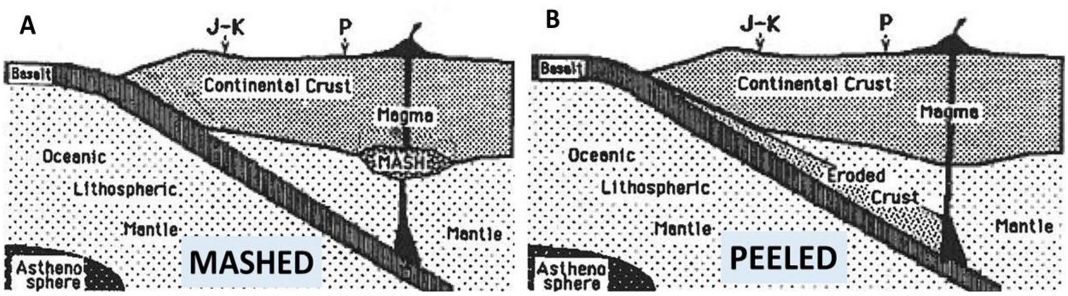

Figure 1. Two alternative explanations for the incorporation of continental crust into Andean magmas [1]. (**A**) MASHED on the left involves Mixing, Assimilation, Storage and Homogenization (MASH) at either the lower crust/mantle boundary or in the crust [2]. (**B**) PEELED on the right involves recycling of subduction eroded crust into the mantle wedge source [3-5]. J-K and P indicate the positon of the Jurassic-Cretaceous and Pliocene plutonic belts, respectively, in the Andes of northern Chile. The recently active volcanic arc is ~250 km east of the Jurassic arc as a result of subduction erosion [6].

In the same way, at the northern end of the Andean SVZ (NSVZ; Figures 2 and 3), where the MASH model was first presented [2], the crust thickens to ≥60 km compared to ≤35 km below the CSVZ, and the isotopic compositions of recently erupted volcanic rocks indicate that they contain greater amount of crustal components [3-5,10,11]. However, the subduction of the Juan Fernández Ridge has caused the subduction angle to flatten, increasing the rate of subduction erosion west of the NSVZ to between 115 to 230 km^3/km/my over the last 10 m.y., during which time the active volcanic arc between 33-34°S migrated ~50 km to the east (Figure 3). Stern [3-5] therefore proposed that crustal components were preferentially incorporated in NSVZ compared to CSVZ magmas by increased rates of subduction erosion and mantle source region contamination by subducted components, and not by intra-crustal MASH processes.

Preprints (www.preprints.org) | NOT PEER-REVIEWED | Posted: 29 July 2019 doi:10.20944/preprints201907.0327.v1

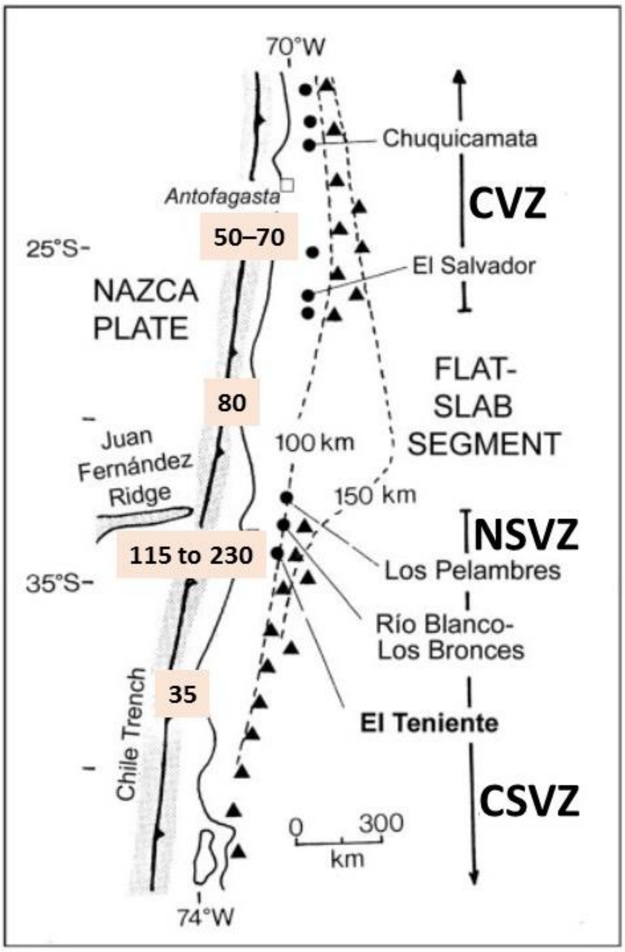

Figure 2. Location of El Teniente and two other giant Late Miocene Cu-Mo deposits, Los Pelambres and Río Blanco-Los Bronces, in the Andes of central Chile. Map also shows tectonic features such as the Chile Trench, which is the boundary between the Nazca and South American plates, the depth in kilometers (100 and 150 km dashed lines) to the Benioff Zone below South America, and the locus of subduction of the Juan Fernández Ridge. This also marks the boundary between the Andean Flat-Slab segment, below which the subduction angle is very low, as indicated by the depths to the upper boundary of the subducted slab, and the northern and central parts of the Andean Southern Volcanic Zone (NSVZ and CSVZ) of active volcanoes, below which subduction angle is steeper. The numbers in the boxes are the estimated rates of subduction erosion in km^3/km/my in each region [5]**.** The map also shows the location of the Central Volcanic Zone (CVZ) and some of the other giant Late Eocene and Early Oligocene Cu-Mo deposits in northern Chile.

Temporal variations in Andean igneous rocks also are not unambiguously related to either changes in crustal thickness or rates of subduction erosion. Below the NSVZ, in the region where the El Teniente deposit formed in the Late Miocene, the crust has thickened and been uplifted since the Middle Miocene [12-20], and Sr, Nd and Pb isotopic data indicate increased proportions of continental crust in the igneous rocks emplaced through time (Figures 4 and 5) [10,21-24]. However, as described above, the southward migration of the locus of subduction of the Juan Fernández Ridge has also caused, during this same time period, flattening of the angle of subduction, >50 km of eastward migration of the volcanic arc, and increased rates of subduction erosion (Figure 3) [3-5,10,25-27].

 doi:10.20944/preprints201907.0327.v1

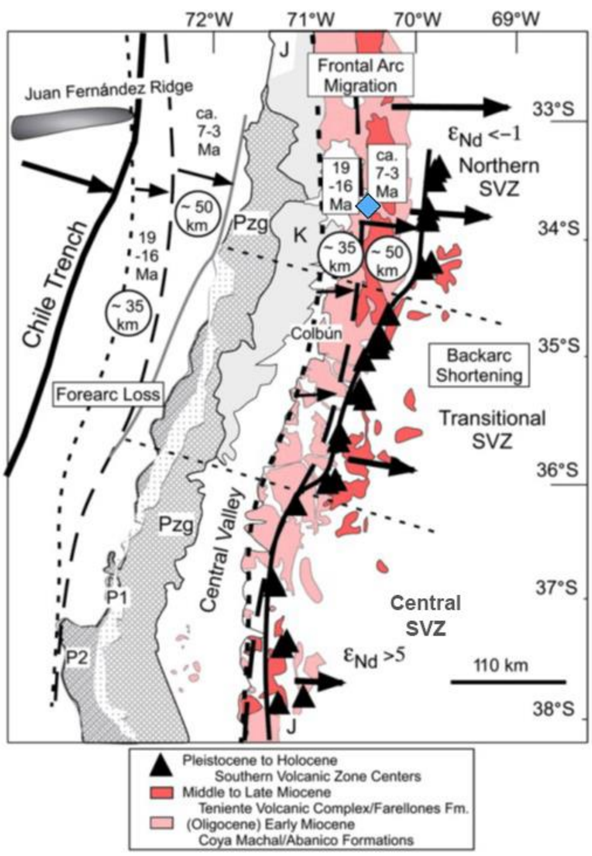

Figure 3. Regional map of central Chile between ~32°S and 38°S, with lines showing correlations of early Miocene to Holocene arc fronts on land and inferred position of corresponding coastlines offshore [10]. Arrows show relative amounts of frontal-arc migration, forearc loss, and backarc shortening. Northwest–southeast trending dashed lines show offsets in the modern volcanic front that separate the Southern Volcanic Zone (SVZ) into the northern, transitional, and central segments [4]. In the active arc region, lines connect outcrop patterns marking early Miocene (pink), middle to late Miocene (red), and SVZ (undashed, connecting Pleistocene to Holocene volcanic centers (triangles)) magmatic fronts. Arrows between the lines indicate inferred distance (given in circles) of frontal-arc migration from 19 to 16 Ma and from 7 to 3 Ma. In the forearc, lines between the trench and the coast show inferred early Miocene (short dashed) and middle to late Miocene (long dashed) coastlines under the assumption that the distance of frontal-arc migration equals the width of missing coast. Arrows between the lines indicate distance (shown in circles) of inferred loss from ca. 19 to 16 Ma. And 7 to 3 Ma. In the backarc, the length and position of arrows show the location and proportional amounts of crustal shortening over the past 20 my inferred from structural profiles. Also shown are other outcrop patterns that have long been used as evidence for forearc subduction erosion along this margin [6]. The first is the northward narrowing and disappearance of the Paleozoic high pressure (P1) and low pressure (P2) paired metamorphic and granitoid (Pzg) belts along the coast. The second is the presence of Jurassic arc rocks (marked by J) along the coast north of 33°S, but inland near the SVZ at ~38°S. K indicates Cretaceous magmatic rocks. ε_{Nd} is +5 for active SVZ volcanoes south of 36°S, and ≤-1 for those in the northern SVZ north of 34°S, as a result of increased mantle source region contamination by subducted crust due to the northward increase in the rate of subduction erosion associated with the subduction of the Juan Fernández Ridge at 33°S [3-5]. El Teniente occurs at the blue diamond

 doi:10.20944/preprints201907.0327.v1

In summary, spatial and temporal variations in geologic factors such as crustal thickness and rates of subduction erosion rates do not unambiguously favor MASH versus source region contamination (Figure 1) in producing the spatial and temporal isotopic variations that indicate increased incorporation of continental crust in some Andean magmas. An alternative approach to distinguish these two processes is geochemical modelling focused specifically on mafic olivine-bearing basaltic rocks clearly derived from the mantle without significant evidence for or possibility of intra-crustal contamination. For instance, to produce the northward increase of $^{87}Sr/^{86}Sr$ from 0.7039 to 0.7050 and decrease in ε_{Nd} from >+5 to <-1 (Figures 3-5) observed in olivine basalts erupted from CSVZ compared to NSVZ volcanoes, would require, because of the relative high Sr = >450 ppm and Nd = 9 ppm of Andean basalts, intra-crustal assimilation (MASH) of >40 wt % of Andean crust (Figure 5) [3,10,21,22]. For NSVZ basalts, with no macro or microscopic evidence of crustal xenoliths or xenocrysts, this is considered to be an unacceptably large amount of crustal assimilation. In contrast, because of the relatively low Sr = 36 ppm and Nd = 1.8 ppm of Andean subarc mantle, these variations could be produced by incorporation in the mantle source region of only 5 wt % more subducted crust and sediment below the NSVZ (Figure 5), where current subduction erosion rates are estimated as between 115 to 230 km^3/km/my (Figure 2), than the 1 wt % estimated to have been incorporated in the mantle below the CSVZ, where subduction erosion rates are estimated as only ~35 km^3/km/my (Figures 2).

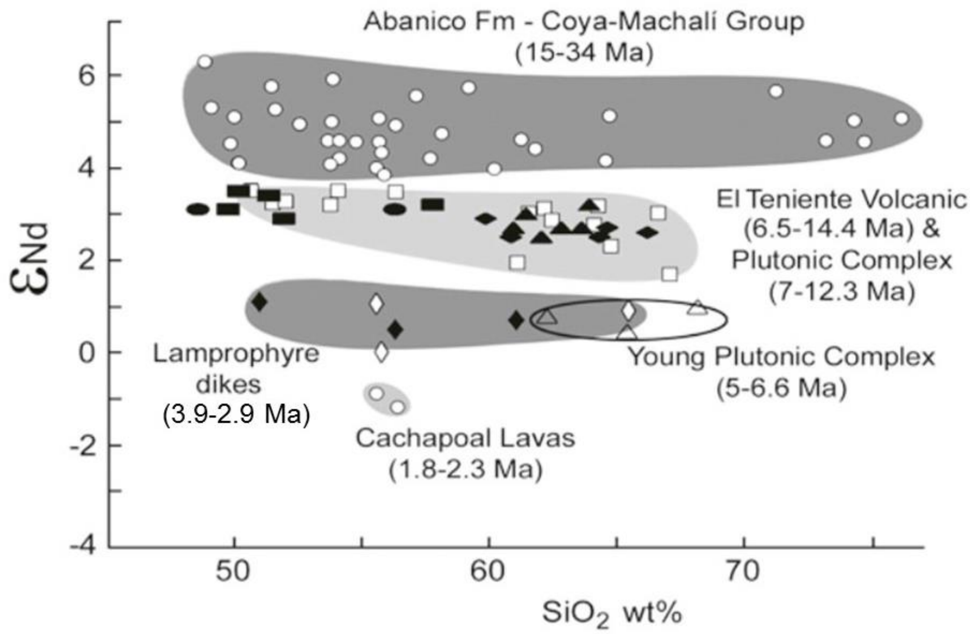

Figure 4. Published values of ε_{Nd} vs SiO_2 (wt %) for igneous rocks of different ages from the transect across the Andes at the latitude of El Teniente (34°S; open symbols [10,14, 17,21-24]), compared with values for samples of the host-rocks in the deposit (filled symbols including the Teniente Mafic Complex (■), Sewell Tonalite (▲), felsic porphyries(♦), and Porphyry A granitoid (●); [23]). Although the youngest felsic plutons in the deposit are the same age (7.1 to 4.6 Ma) as rocks from the regionally defined Younger Plutonic Complex (6.6 to 5 Ma; [10]) they are isotopically similar to the older host-rocks of the deposit as well as to Teniente Volcanic and Plutonic Complex rocks.

Preprints (www.preprints.org) | NOT PEER-REVIEWED | Posted: 29 July 2019 doi:10.20944/preprints201907.0327.v1

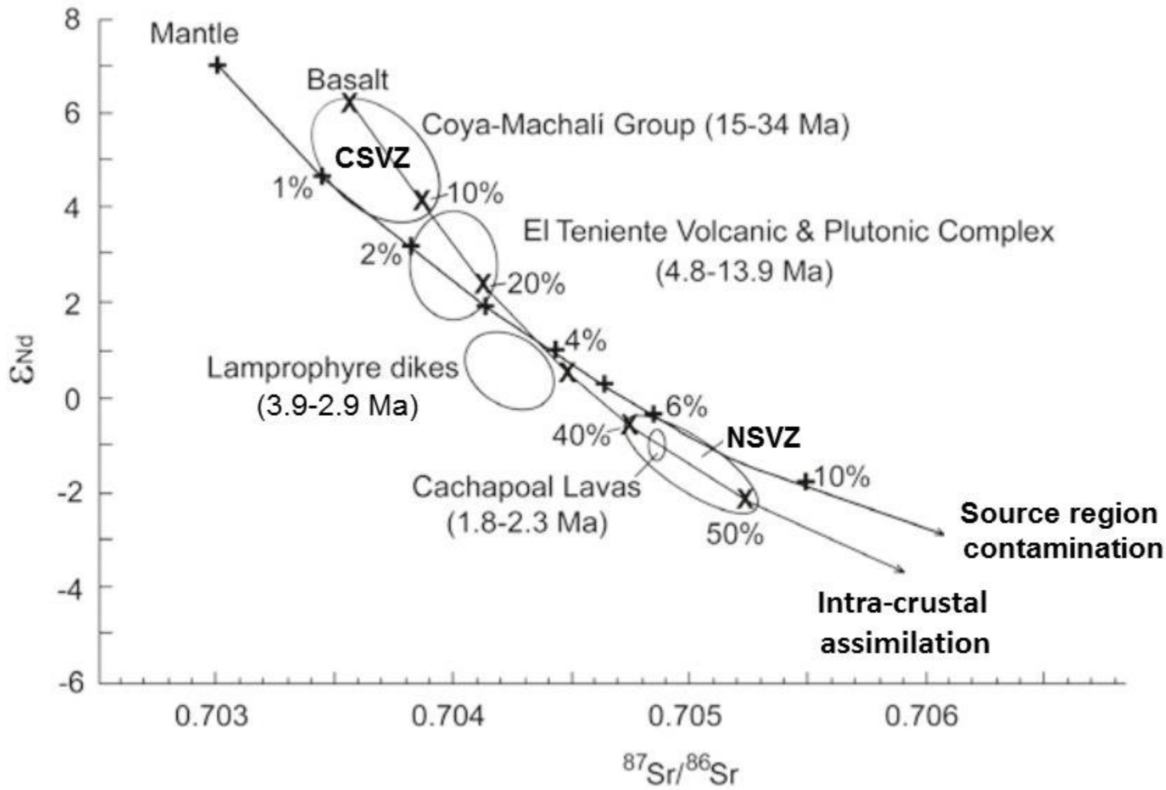

Figure 5. Sr versus Nd isotopic values of the various groups of igneous rocks of different ages across a transect of the Andes at the latitude of El Teniente (34°S; fields and data sources from Figure 4). The figure illustrates both a source region contamination model of primitive mantle (Sr=36 ppm with $^{87}Sr/^{86}Sr$=0.703 and Nd=1.8 ppm with ε_{Nd}= +7; [21]) mixed with various proportion of subducted crust and sediment (Sr=380 ppm with $^{87}Sr/^{86}Sr$=0.70763 and Nd=42.3 ppm with ε_{Nd}= -5.1), and also a MASH model for a Coya-Machalí basalt (Sr=450 ppm with $^{87}Sr/^{86}Sr$= 0.7035 and Nd=9 ppm with ε_{Nd}= +6) assimilating various proportion of Paleozoic-Triassic Andean granite basement (Sr=350 ppm with $^{87}Sr/^{86}Sr$=0.7075 and Nd=20 ppm with ε_{Nd}= -6; [10]) Both models reproduce the isotopic compositions of the progressively younger rocks in the transect, but the latter model requires assimilation of unacceptably high proportions of granite crust and is inconsistent with generation of primitive low SiO_2 olivine-bearing mafic rocks in each age group, as well as the increasingly higher Sr content of the progressively younger rocks, which is due instead to decreasing degrees of partial mantle melting [3-5,10], consistent with decreasing volume of magmas erupted through time at this latitude in the Andes.

Exactly similar temporal isotopic changes as those observed between recently erupted CSVZ and NSVZ basalts occurred between the Miocene and Pliocene in igneous rocks associated with the giant El Teniente Cu-Mo deposit (Figures 2-5) [21-23]. As a contribution to the understanding of Andean magmagenesis its implications for the formation of the El Teniente ore deposit, we have determined Hf isotopes in igneous rocks ranging in age from ≥8.9 to 2.3 Ma from the area of the deposit. These samples (Table 1) include an olivine basalts (8.9 Ma), an olivine lamprophyre (3.1 Ma), and an olivine-bearing basaltic andesites (2.3 Ma), as well as other mafic and felsic plutons associated with the deposit. The data obtained provide information about the temporal evolution of their magmatic sources from the Late Miocene to Pliocene, and constrain the relative role of MASH and mantle source region contamination processes in the generation of Andean magmas.

Preprints (www.preprints.org) | NOT PEER-REVIEWED | Posted: 29 July 2019 doi:10.20944/preprints201907.0327.v1

Table 1. Samples analyzed [21-23,37].

sample #	rock type	age Ma	SiO_2	$^{87}Sr/^{86}Sr$	$^{143}Nd/^{144}Nd$	ε_{Nd}	ε_{Hf}[37]
Late Miocene (≥8.9 Ma) mafic host rocks							
EX-2004-04	ol basalt	8.9	51.9	0.70405	0.512782	2.9	
1411-1630	gabbro	≥8.9	51.1	0.70396	0.512818	3.5	
540-2082	basalt	≥8.9	51.3	0.70404	0.512813	3.4	
QT-4	basalt	≥8.9	49.7	0.70421	0.512798	3.1	
Late Miocene to Early Pliocene (7.1 to 4.8 Ma) felsic plutonic rocks							
Ttc5	Sewell tonalite	7.1	63.7	0.70386	0.512770	2.7	7.9
1473-970	Porphyry A	5.7	48.5	0.70409	0.512799	3.1	
1446-266	Porphyry A	5.7	56.3	0.70406	0.512795	3.1	7.7
1300-403	Teniente dacite	5.3	66.3	0.70402	0.512762	2.6	7.2
1394-92	latite dike	4.8	60.9	0.70405	0.512785	2.5	6.9
Pliocene (3.8 to 2.3) lamprophyres and basaltic andesites							
Ttc1	hbl lamprophyre	3.8	56.3	0.70425	0.512660	0.7	
AS-2003-1	ol lamprophyre	3.1	51.3	0.70425	0.512700	1.2	
PVF1	ol basaltic andesite	2.3	55.6	0.70485	0.512580	-1.1	

2. Geologic Background

2.1. El Teniente Cu-Mo deposit

The giant El Teniente Cu-Mo deposit, located in central Chile (34°05'S, 70°21'W; Figures 2 and 3) is one of the largest such deposits in the world [28-38]. It is the southernmost in a belt of Late Miocene giant Cu-Mo deposits which also include Los Pelambres and Río Blanco-Los Bronces [39,40]. El Teniente has been described as a porphyry deposit formed around the central Teniente Dacite Porphyry dike (Figure 6) [30], or alternatively as a magmatic-hydrothermal breccia deposit formed either in association with the intrusion of dacite to diorite dikes [36] or by the generation of multiple large mineralized breccias, including the central Braden breccia pipe, by exsolution of high-temperature mineral-rich magmatic-hydrothermal fluids from the roof of an underlying large, long-lived and vertically stratified magma chamber recharged from below by mantle-derived magmas [23,32,33,38]. The two other Miocene deposits in this belt are also characterized by the presence of multiple large mineralized magmatic-hydrothermal breccias [38-42].

Pb, S, O and H isotopic studies of the igneous rocks and ore minerals in the deposit indicate that El Teniente is clearly an orthomagmatic deposit, with Cu, Mo and S being derived from the associated igneous rocks [32,33,39,43-45]. Igneous rocks spatially related with the deposit range in age from mid Tertiary to Pliocene. Over this time period the volume of magmatic rocks decreased progressively [22,23,38,39], and in the Pliocene the locus of Andean arc magmatism at the latitude of El Teniente (34°S), near the current northern end of the Andean Southern Volcanic Zone (NSVZ; Figures 2 and 3), migrated ~50 km to the east as subduction angle flattened [25]. This, we suggest, was due to the southward migration of the locus of subduction of the Juan Fernández Ridge (21,25-27,38,39].

Preprints (www.preprints.org) | NOT PEER-REVIEWED | Posted: 29 July 2019 doi:10.20944/preprints201907.0327.v1

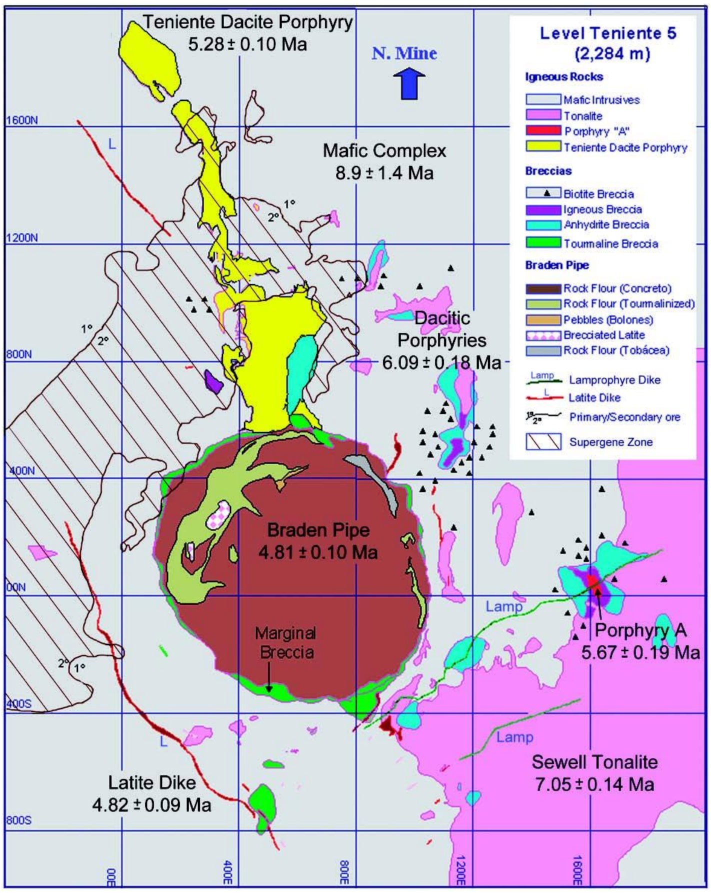

Figure 6. Geological map of level Teniente 5 (2284 m above sea level) in the mine [32,33]. The Dacitic Porphyries north of the Sewell Tonalite, are mapped as a distal portion of this pluton, although they are younger [34] and have an independent origin [36]. The spatial extent of biotite breccias is projected onto this level from where they have been mapped between levels Teniente 4 and 8.

The igneous rock in the vicinity of El Teniente include continental volcanic rocks, up to 3300 m thick, of the Oligocene to Early Miocene (≥15 Ma) Coya-Machali (or Abanico; Figure 3) Fm. [15,46,47], erupted above thin (<30 km) crust, or in a transtensional intra-arc basin [48]. These formed by relatively high degrees of partial melting of subarc mantle modified to a small degree by the influx from below of slab-derived components [10,17,46]. This is indicated by their low La/Yb ratios (2-6), as well as their low initial $^{87}Sr/^{86}Sr$ (0.7033-0.7039) and high ε_{Nd} (+6.5 to +4; Figures 4 and 5). Although the Coya-Machali Formation volcanic rocks do not crop out either within or in the immediate vicinity of the El Teniente deposit (Figures 3 and 6), these rocks occur both to the west and the east of the deposit, and they almost certainly also occur at depth below the deposit.

Extrusive rocks of the Miocene Farellones Formation, locally referred to as the Teniente Volcanic Complex [10], are the oldest rocks exposed in the immediate area surrounding the deposit (Figure 3). The Farellones Formation, a sequence of >2500 m of lavas, volcanoclastic rocks, dikes, sills and stocks of basaltic to rhyolitic composition, was erupted after an Early Miocene (19-16 Ma episode of crustal deformation, thickening and uplift [10,14]. The Teniente Volcanic Complex near the deposit has been correlated with the upper part of this formation and dated between 14.4 and 6.5 Ma [10,31]. No extrusive rocks with ages less than 6.5 Ma have been found within the El Teniente deposit.

Preprints (www.preprints.org) | NOT PEER-REVIEWED | Posted: 29 July 2019 doi:10.20944/preprints201907.0327.v1

The Teniente Volcanic Complex consists of tholeiitic to calc-alkaline extrusive rocks, which plot in the medium to high-K group of convergent plate boundary arc magmas [10]. Mafic rocks of the Teniente Volcanic Complex generally have higher La/Yb (4-9) compared with rocks of the older Coya-Machali Formation, and mafic, intermediate and silicic rocks also have higher initial $^{87}Sr/^{86}Sr$ (0.7039-0.7041; Figure 5) and lower initial ε_{Nd} (+2.7 to +3.6; Figures 4 and 5). These differences are interpreted to represent a change from magma genesis below relatively thin continental crust during the mid-Tertiary, when the Coya-Machali Formation was generated, to conditions of thickened continental crust when the Teniente Volcanic Complex formed in the Middle to Late Miocene.

The extrusive rocks of the Teniente Volcanic Complex were intruded during a Late Miocene (9-5 Ma) episode of further crustal deformation, thickening and uplift, between ~8.9 and 4.6 Ma [10,14,31,34,48], by gabbro, diabase, diorite, tonalite, latite, and dacite porphyry plutons of the Teniente Plutonic Complex. Within the immediate area of the deposit (Figure 6) these include 1) the >50 km^3 Teniente Mafic Complex (8.9 ± 2.4 Ma) of mafic intrusives with the form of a laccolith 2000 m thick in the center of the deposit; 2) the equigranular holocrystalline Sewell Tonalite complex (7.05± 0.14 Ma), with an estimated volume of ~30 km^3 [23]; and 3) a series of much smaller volume (<1 km each) dacite and diorite porphyries (6.09±0.18 Ma), the unusual Cu- and S-rich anhydrite-bearing Porphyry A stock (5.67±0.19 Ma) [49], the Teniente Dacite Porphyry dike (5.28±0.10 Ma), a few latite dikes (4.82±0.09 Ma), and finally a small dacite porphyry (4.58±0.10 Ma). These intrusive rocks have isotopic compositions similar to Teniente Volcanic Complex extrusives (Figures 4 and 5).

Multiple Cu-mineralized magmatic-hydrothermal breccia pipes were emplaced into these plutonic rocks during the same time period as the felsic porphyry intrusions, between at least 6.3 and 4.4 Ma (Figure 6). Post-mineralization phases include high-MgO (≥7.50 wt %) olivine (Fo88) and hornblende lamprophyres (3.8 to 2.9 Ma) [10,22,31,34] and olivine (Fo64) basaltic andesite (MgO≥4.5 wt %) lavas in the valley of the Cachapoal river just west of the El Teniente deposit (2.3 Ma) [21]. After this the locus of Andean arc magmatism migrated eastwards ~50 km (Figure 3).

2.2. Previous Hf isotopic studies

Hf isotopes have previously been determined in zircons from felsic plutons both within [37] and in the near vicinity [50] of the El Teniente deposit (Figure 7). The Hf isotopic composition of zircons in six samples of felsic plutons within the deposit, that range in age from 7.1 to 4.8 Ma, have overall high initial average of ε_{Hf} = +7.4 ± 1.2 and range from +6 to +10 (Table 1), which rules out significant crustal contamination [37]. There was little change in these compositions during this time, but the older four plutons (7.1 to 6.1 Ma) average ε_{Hf} = +7.8, while the younger Teniente Dacite Porphyry (5.3 Ma) has ε_{Hf} = +7.2 and the youngest latite dike (4.8 Ma) has ε_{Hf} = +6.9 (Table 1), so some small but significant temporal change, with decreasing ε_{Hf} through time, is apparent.

Hf isotopic compositions were also determined in four barren Middle and Late Miocene plutonic complexes in the vicinity of El Teniente [50]. These can be divided into an older group (~15 Ma) and a younger group (10 to 12 Ma), both groups being older than the felsic plutons within the El Teniente deposit (Figure 7). The older group is characterized by quartz monzogabbroic compositions with 54.0 to 57.5 wt % SiO_2, while the younger group are quartz monzodioritic with higher SiO_2 from 61.6 to 66.8 wt %. ε_{Hf} for the older group ranges from +9.8 to +13.7 and averages +11.6 (Figure 7), while ε_{Hf} for the younger group has a lower range of +7.6 to +8.5 and lower average of +8.0. These differences are also associated with increasing ε_{Os} from +32 to +160 for the older compared to the

 doi:10.20944/preprints201907.0327.v1

younger group. Both the Hf and Os isotopic data suggests increasing incorporation of crustal components with time, and the younger plutons, which have higher SiO_2, are noteworthy for the presence of abundant mafic enclaves indicating intra-crustal (MASH) assimilation on a macroscopic scale. These are absent from the older plutonic group which have more primitive isotopic compositions and lower SiO_2.

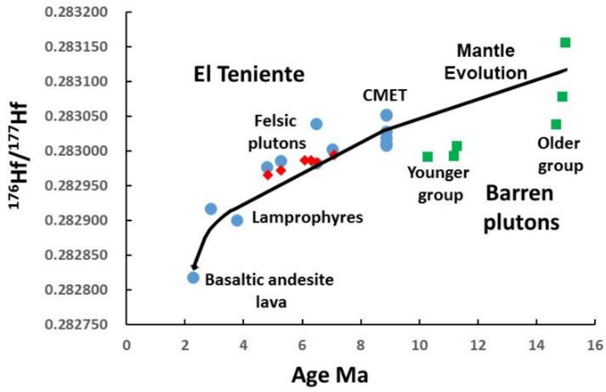

Figure 7. $^{176}Hf/^{177}Hf$ versus age (Ma) for samples from El Teniente (blue circles from Table 2; red diamonds from [37]) and Middle Miocene barren plutons in the same general area (green squares from [50]). Mantle isotopic evolution line is draw from average of older group of Middle Miocene barren plutons through Late Miocene Teniente Mafic Complex (CMET) olivine basalts and gabbros, to olivine lamprophyres and olivine-bearing basaltic andesites, ignoring the younger group of barren plutons because these have macroscopic evidence for intra-crustal assimilation [50]. The amount of subducted crust plus sediment added to the mantle to generate this line is indicated in Figure 9.

Hf and Nd isotopic compositions have also been determined for five Late Miocene to Pliocene (8.3 to ~3 Ma) plutons from the Eastern Principal Cordillera ~40 km east of El Teniente (Figure 8) [24]. These have lower more radiogenic ε_{Hf} (+4 to -4) and ε_{Nd} (+3 to 0) than the felsic plutons in El Teniente. Crustal-contamination (MASH) processes involving assimilation of Paleozoic and Mesozoic basement rocks are evidently involved in the genesis of the igneous rocks from the Eastern Cordillera (Figure 8), both because some contain zircon crystal with older (Paleozoic) inherited cores and others have wide ranges (+1 to -4) of zircon ε_{Hf} values [24]. We agree with this interpretation. However, it has also been suggested[24], based on the low ε_{Nd} values of the Pliocene olivine lamprophyres (+1.2 to +0.7) and olivine-bearing basaltic andesites (-1.1; Figures 4 and 5; Table 1; [21-23]) emplaced in the Western Cordillera in the vicinity of El Teniente, which are similar to those in the Pliocene plutons of the Eastern Cordillera, that these low ε_{Nd} values reflects a westward propagation of the Eastern Cordillera magmatic isotopic signatures, caused by westward thrusting and material transport of the Eastern Cordillera basement under the Western Cordillera in the Pliocene (Figure 8). We disagree with this interpretation as it fails to take into account the fact that the Pliocene high-Mg olivine lamprophyres, as well as the olivine-bearing basaltic andesite lavas, are likely to be mantle-derived, without significant crustal contamination. For high-Mg olivine lamprophyres in general, an origin by hydrous (6-16 wt % H_2O) melting of mantle has been suggested [51-55]. As discussed in more detail below, we therefore interpret these temporal change in both ε_{Hf} and ε_{Nd} to lower more radiogenic values as reflecting a progressive change in mantle composition due to subduction of increased proportions of continental crust, and not to intra-crustal (MASH) contamination processes.

Preprints (www.preprints.org) | NOT PEER-REVIEWED | Posted: 29 July 2019 doi:10.20944/preprints201907.0327.v1

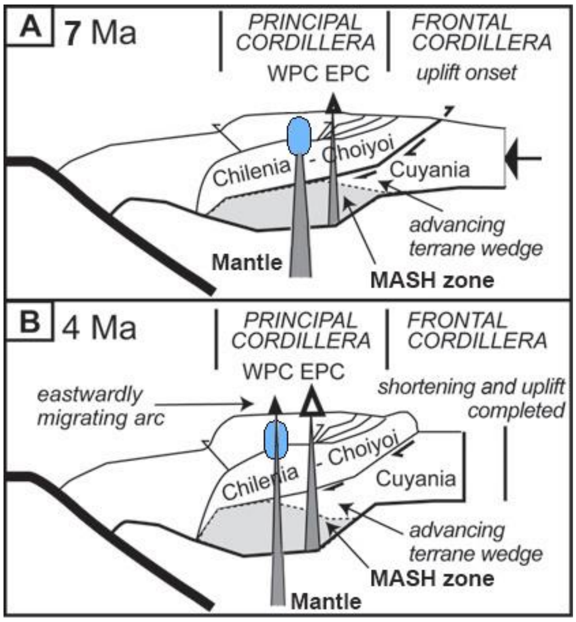

Figure 8. Schematic profiles [18-20,24] of crustal evolution of the Andes of central Chile and Argentina at 7 Ma (A) and 4 Ma (B). Evolution is characterized by increased shortening rates along the eastern flank of the orogenic belt after 7 Ma, where the Chilenia-Choiyoi block overrides the Cuyania terrane, producing uplift of the Frontal Cordillera. This also produced increasing crustal thickness which led to uplift of the entire belt. Deformation amounts suggest that the Cuyania block descended immediately below the eastern part of the magmatic arc, changing composition of the base of the crust and thus changing the crustal magmatic source (MASH zone) below the Eastern Principle Cordillera (EPC). However, below the Western Principle Cordillera, magmas continued to rise from the mantle without intra-crustal assimilation in a MASH zone. After 7 Ma, these magmas did not reach the surface, but were mixed, stored and homogenized in a large magma chamber (blue) below El Teniente. Within this chamber the felsic plutons of the deposit developed without crustal assimilation and above it the mineralized breccias in the deposit were emplaced (see Figure 10). As subduction angle flattened and magma supply from the mantle decreased this chamber solidified. After 4 Ma, high-MgO olivine lamprophyres and olivine-bearing basaltic andesites, derived from a mantle hydrated and isotopically modified by increased proportions of subducted crust and sediment (Figure 7), rose through the now crystallized magma chamber, without any intra-crustal assimilation, to form dikes and lavas.

Finally, ε_{Hf} values between +6.9 to + 9.6 were determined for 8 plutonic rocks between the ages of 28.1 and 11.5 Ma from the region north of El Teniente between 32-33°S [47]. The oldest sample, a dacite sill (sample Ab-143; 28.1 Ma), which has $(^{87}Sr/^{86}Sr)_i$ = 0.70661 and is likely to have assimilated crustal material, has lower ε_{Hf} of +7.8 than younger (22.2-17.7 Ma) gabbro, microgabbro and granodiorite samples which average ε_{Hf} of +8.9. All the still younger plutons have lower ε_{Hf} and the youngest (11.5 Ma; sample Z-132) has an ε_{Hf} of +7.0. This suggest decreasing ε_{Hf} with time beginning after ~17 Ma, and possibly before this time. Since these samples are all north of the current locus of subduction of the Juan Fernández Ridge, in an area where ridge subduction, decreasing subduction angle, eastward arc migration and increased rates of subduction erosion all happened earlier than at the latitude of El Teniente, we do not consider them appropriate for evaluating the temporal evolution of the mantle source of El Teniente magmatic rocks.

Preprints (www.preprints.org) | NOT PEER-REVIEWED | Posted: 29 July 2019 doi:10.20944/preprints201907.0327.v1

3. Samples and Methods

Twelve samples were selected for Hf-isotopic analysis (Table 1). These range in age from ≥8.9 to 2.3 Ma and include 1) four samples from the Teniente Mafic Complex, including one olivine (Fo74) basalt, one gabbro and two other olivine-free basalts; 2) five syn-mineralization felsic intrusions that range in age from 7.1 to 4.8 Ma, including four samples previously analyzed for Hf-isotopes in zircon [37]; and 3) three post-mineralization samples that range in age from 3.8 to 2.3 Ma, including one high-MgO (7.9 wt %; Ni ~190 and Cr ~390 ppm) olivine (Fo88) lamprophyre [22] and one olivine-bearing (Fo64) basaltic andesite. All the samples have been previously analyzed for major and trace element contents and Sr and Nd isotopic compositions (Table 1) [21-23].

Ground sample weighing ~200 mg was decomposed in 15 ml screw-top Savillex Teflon® vials with a 1:1 mixture of 27 N HF and 16 N HNO_3 at ~150°C for 5 days. The sample solution was evaporated to incipient dryness and redissolved first by 2 ml 4 N HCl and then by 1 N HCl. The dried sample was then taken into solution by 1 ml 2N HCl and 8 ml 6 N HCl–0.2 N HF prior to chemical separation. Hafnium was separated from the matrix elements by two columns packed with Ln-spec resin (50–100 μm) from Eichrom Industries. Major elements and REE were eluted by 3 N HCl and 6 N HCl, and then Ti and Zr were eluted using a 2 N HCl–0.1 N HF mixture. Hafnium was collected from the column with 2 N HCl and 0.2 N HF, and was then evaporated to incipient dryness and taken up by 2 N HCl–0.2 N HF. The chromatographic procedures are repeated again on the same column for further purification. Hafnium isotopes were measured on Nu Plasma II multi-collector ICP-MS connected to a Aridus II desolvator and an enhanced sensitivity system with Ni 325-294 skimmer cone and Ni 319-646 sampler cone. The measured $^{176}Hf/^{177}Hf$ values were normalized for mass fractionation based on $^{179}Hf/^{177}Hf = 0.7325$. Long-term mean value for the Hf standard JMC475 in the laboratory is $^{176}Hf/^{177}Hf = 0.282164 \pm 8$ (n = 55). The $^{176}Lu/^{177}Hf$ ratio was calculated from the Lu and Hf contents determined by ICP-MS techniques by Activations Laboratories (Canada).

4. Results

The ε_{Hf} determined on the bulk-rock samples of the 7.1 to 4.8 Ma felsic plutons are similar within analytical error to those determined previously on zircons for the same plutons [37]. Although Muñoz et al. [37] concluded that there was no change in ε_{Hf} among these plutons, the new data for samples formed over the larger ~6.6 m.y. interval from ≥8.9 to 2.3 Ma indicates that there was a clear progressive decrease in ε_{Hf} with decreasing age (Figure 7). The ε_{Hf} for the twelve samples ranges from an average of +9.1 for the four samples of ≥8.9 Ma Teniente Mafic Complex basalts and gabbros down to +1.6 for the 2.3 Ma olivine-bearing basaltic andesite lava flow which is the last manifestation of magmatic activity in the region of El Teniente prior to the eastward migration of the volcanic arc (Table 2). This implies a drop of 7.5 ε_{Hf} units over this 6.6 m.y. interval.

Muñoz et al. [37] also suggested that the full ε_{Hf} range of +6 to +10 of the 7.1 to 4.8 Ma felsic plutons is "identical to preceding Cenozoic barren magmatic activity in Central Chile." However, although their average ε_{Hf} values of +6.9 to +7.9 (Table 1) are in fact somewhat lower than the younger group (10-12 Ma) of barren plutons, for which macroscopic and Os isotopic evidence of upper crustal assimilation has been documented, they are significantly lower than the older group (~15 Ma; Figure 7). When the ε_{Hf} of the older ~15 Ma barren plutons in the region, which average +11.6 [50], are taken into account, it is clear that ε_{Hf} values have not remained constant through time (Figure 7). In fact,

Preprints (www.preprints.org) | NOT PEER-REVIEWED | Posted: 29 July 2019 doi:10.20944/preprints201907.0327.v1

there has been an overall decrease of 10 ε_{Hf} units for igneous rocks emplaced in the vicinity of El Teniente in the 12.7 m.y. period from the Middle Miocene to the Pliocene.

Table 2. Hf isotopes of the El Teniente samples.

Sample	Lu (ppm)	Hf (ppm)	$^{176}Lu/^{177}Hf$	$^{176}Hf/^{177}Hf$	$2\sigma x10^{-6}$	$(^{176}Hf/^{177}Hf)i$	$\varepsilon_{Hf(t)}$
Late Miocene (≥8.9 Ma) pre-mineralization mafic host rocks							
EX-2004-04	0.25	2.7	0.0131	0.2830107	3.3	0.283009	8.6
1411-1630	0.21	1.7	0.0175	0.2830506	6.1	0.283048	9.9
1411-1630 dup	0.21	1.7	0.0175	0.2830512	3.6	0.283048	10.0
540-2082	0.24	1.9	0.0179	0.2830072	3.9	0.283004	8.4
540-2082 dup	0.24	1.9	0.0179	0.2830272	4.2	0.283024	9.1
QT-4	0.25	2.5	0.0142	0.2830179	3.4	0.283016	8.8
Late Miocene to Early Pliocene (7.1 to 4.8 Ma) syn-mineralization felsic plutonic rocks							
Ttc-5	0.11	3.2	0.0049	0.2830014	11	0.283001	8.2
1473-970	0.16	2.8	0.0081	0.2830385	6.0	0.283038	9.5
1446-266	0.11	3.9	0.0040	0.2829811	7.5	0.282981	7.5
1300-403	0.06	2.4	0.0036	0.2829843	3.7	0.282984	7.6
1394-92	0.07	2.9	0.0034	0.2829762	2.8	0.282976	7.3
Pliocene (3.8 to 2.3) post-mineralization olivine lamprophyres and basaltic andesites							
Ttc1	0.12	3.5	0.0049	0.2828997	3.8	0.282899	4.6
AS-2003-1	0.18	3.1	0.0082	0.2829158	3.1	0.282915	5.1
PVF1	0.30	5.0	0.0085	0.2828165	2.3	0.282816	1.6

5. Discussion

5.1. Andean magmagenesis

The observed 10 ε_{Hf} unit decrease for igneous rocks emplaced in the vicinity of El Teniente in the 12.7 m.y. period from the Middle Miocene to the Pliocene is consistent with decreasing $\varepsilon_{Nd(t)}$ from +5 to -1.1, increasing $^{87}Sr/^{86}Sr(i)$ from 0.70376 to 0.70485, and increasing $^{206}Pb/^{204}Pb$ from 18.55 to 18.68 determined for these same samples (Figures 4 and 5) [21-23]. These variations imply increasing incorporation of continental crust through time in the magmas that formed these rocks.

The fact that the samples include mantle-derived olivine basalts and high-Mg olivine lamprophyres suggests that these continental components were incorporated into their mantle source, and not by intra-crustal contamination (MASH). This suggestion is supported by two other lines of evidence. One is that for all the rocks of variable SiO_2 content within the igneous associations of specific ages identified in the area of El Teniente, the isotopic compositions do not vary as SiO_2 increases (Figure 4). The isotopic compositions of the different associations vary through time, but not as a function of SiO_2. This implies that crystal fractionation processes are not combined with intra-crustal assimilation in the generation of the range of rocks from basalts through rhyolites formed during each of these successive magmatic events. Second, models of intra-crustal assimilation (MASH) for Sr and Nd isotopes (Figure 5; [21-23]) indicate that relatively large proportions (>40 wt %) of crust must be assimilated to produce the Sr and Nd isotopic changes observed between mid Tertiary basalts and Pliocene olivine lamprophyres and olivine-bearing basaltic andesites. This is

Preprints (www.preprints.org) | NOT PEER-REVIEWED | Posted: 29 July 2019 doi:10.20944/preprints201907.0327.v1

considered to be an unacceptably large amount of crust to be assimilated in olivine-bearing mafic magmas.

In contrast, models of mantle source region contamination by subducted crustal components indicates that the Sr and Nd isotopic evolution of the subarc mantle source of the mafic magmas erupted in the vicinity of El Teniente between the mid Tertiary and Pliocene can be produced by the incorporation of increased, but still relatively small proportions of subducted crust and sediment (Figure 5; 3, 10,21-23). Mid Tertiary Coya-Machali group mafic volcanic rocks require the addition to a primitive subarc mantle of only 1 wt % subducted crust and sediment, while Pliocene olivine lamprophyres and basaltic andesites require the addition of between 4-6 wt % subducted crust to produce an appropriately isotopically modified mantle source.

The difference between these intra-crustal assimilation and mantle source region contamination models reflects the relatively high Sr (450 ppm) and Nd (9 ppm) contents of a basalt relative to the crust being assimilated, thus requiring a relatively large proportion of crust to produce the appropriate isotopic leverage. In contrast the low Sr (36 ppm) and Nd (1.8 ppm) contents of the mantle allows a much smaller proportion of subducted crust and sediment to produce the appropriate isotopic leverage (Figure 5; [3-5,10,21-23]. For the Hf isotopic system, the same logic applies. The olivine basalts and gabbros of the Teniente Mafic Complex contain an average of 2 ppm Hf (Table 2), while average upper continental crust contains 5.3 ppm (Table 3) and bulk continental crust 3.7 ppm Hf [56]. In contrast, primitive mantle contains only 0.28 ppm Hf [57], so the proportion of crust needed to modify the Hf isotopic composition of the mantle is small compared to that needed to be assimilated by a basalt.

Since the mantle source region contamination model better explains the Sr and Nd isotopic evolution through time of the same olivine-bearing mafic rocks that we have analyzed for Hf isotopes, we also interpret the temporal change in their Hf isotopic compositions to reflect the isotopic evolution of their mantle source affected by increased incorporation of subducted crust and sediment. To quantitatively evaluate the amount of source region contamination to produce these Hf isotopic variations is complicated for two reasons. The first is the inherent complexities involved in subduction zone magmatism, such as the amounts of pelagic, terrigenous and tectonically eroded continental crust being subducted, and the uncertainty in the processes of transfer of these components into the overlying mantle wedge by either dehydration and volatile transport, melting or diapiric uprise of these low density materials. The second is that information is not available for the Hf contents and isotopic compositions of all these different components relevant to magmagenesis in the vicinity of El Teniente, in particular for the coastal and off shore Paleozoic and early Mesozoic crustal rocks being tectonically eroded and subducted.

In the central Mexican magmatic belt, west of where subduction erosion rates are estimated as 79-88 km^3/km/my, and where Hf concentration and isotopic data are available for both pelagic and terrigenous sediment, as well as coastal continental rocks, Straub et al. [58] concluded that tectonically eroded continental crust, consisting of coastal and off-shore granodiorite plutons, was the dominant control on the isotopic composition of the calc-alkaline arc magmas, and that neither intra-crustal assimilation nor subducted trench sediment played a significant role in the genesis of these magmas. For the El Teniente rocks, we calculated a model assuming for Hf contents the average estimated values for primitive mantle and the average upper crust for the subducted crust and sediment, as well as a low crustal $^{176}Hf/^{177}Hf$ isotopic ratio similar to that determined by Straub et al. [58] for

Mexican basement biotite gneisses (Table 3). This model can generate results (Figures 7 and 9) consistent with those previously determined for the Sr and Nd isotopic systems for which more published values for the materials involved in Andean magmagenesis are available [10,21-23]. These models indicate that the addition of 1 wt % subducted crust and sediment can produce an isotopically modified mantle appropriate for the generation of the mid Tertiary Coya-Machali basalts. Addition of progressively greater amounts of 2, 4 and 6 wt % subducted crust and sediment is required to further modifiy the mantle to produce the Late Miocene Teniente Mafic Complex olivine basalts and gabbros, the Pliocene olivine lamprophyres and younger Pliocene basaltic andesites, respectively.

Table 3. Parameters used for the mantle modified by subducted crust+sediment model [22].

	Mantle	Crust + Sediment
Sr ppm	36	380
$^{87}Sr/^{86}Sr$	0.7030	0.70763
Nd ppm	1.8	42.3
$^{143}Nd/^{144}Nd$	0.51300	0.51235
Hf ppm	0.28	5.3
$^{176}Hf/^{177}Hf$	0.28320	0.28256

What can be said unequivocally in support of this model of the isotopic evolution of the subarc mantle underlying El Teniente is that the rate of subduction erosion and amount of Paleozoic and early Mesozoic crust being subducted did increase as the locus of subduction of the Juan Fernández Ridge migrated southward. Prior to impingement of the ridge on the northern end of the SVZ, subduction erosion rates may have been similar to those estimated presently for the central SVZ of 35 km^3/km/my (Figure 2; [5]). Over the last ~10 m.y., as the ridge approached it current position at the northern end of the SVZ (Figures 2 and 3; [26,27]), rates of subduction erosion west of El Teniente increased to possibly as high as between 115 to 230 km^3/km/my [5]. This increased rate of subduction erosion must be considered as the most probable cause for the increased crustal Hf, Sr, Nd and Pb isotopic signatures in the igneous rocks associated with the El Teniente deposit through time.

A second important factor that changed over the same time period, was that the angle of subduction decreased, thus contributing, along with subduction erosion, to the ~50 km eastward migration of the Andean arc in the Pliocene (Figure 3; [10,25]). Decreasing subduction angle reduced the volume of the subarc mantle wedge and resulted in a progressive decrease in the volume of magmas being produced prior to arc migration. Even if the amount of crustal components transferred from the subducted slab into the mantle wedge remained the same through time, which it didn't since subduction erosion rates increased, the decreasing volume of the wedge would result in these components becoming progressively more significant within the wedge. Stern [3-5] and Kay et al. [10] have shown that the decreasing volume of magma erupted in the vicinity of El Teniente through time from the mid Tertiary to Pliocene is consistent with decreasing percent of mantle partial melting as the angle of subduction decreased. This resulted in increasing Sr contents, from 450 to 700-900 ppm in association with increasing $^{87}Sr/^{86}Sr$ ratios in the sequence of mid Tertiary basalts to Pliocene olivine bearing mantle-derived lamprophyres [22]. Decreased degrees of mantle partial melting may also explain the somewhat higher Hf contents of the small volume of Pliocene olivine lamprophyres (>3 ppm) and basaltic andesite lavas (5 ppm) compared to the older Teniente Mafic Complex olivine

 doi:10.20944/preprints201907.0327.v1

basalts and gabbros (2 ppm; Table 2). Lamprophyres in general have been attributed to small degrees, relative to basalts, of partial melting of hydrated (6 to 16 wt % H_2O) mantle [51-55], H_2O being one of the subducted components likely to increase in significance in the mantle wedge as mantle volume decreases.

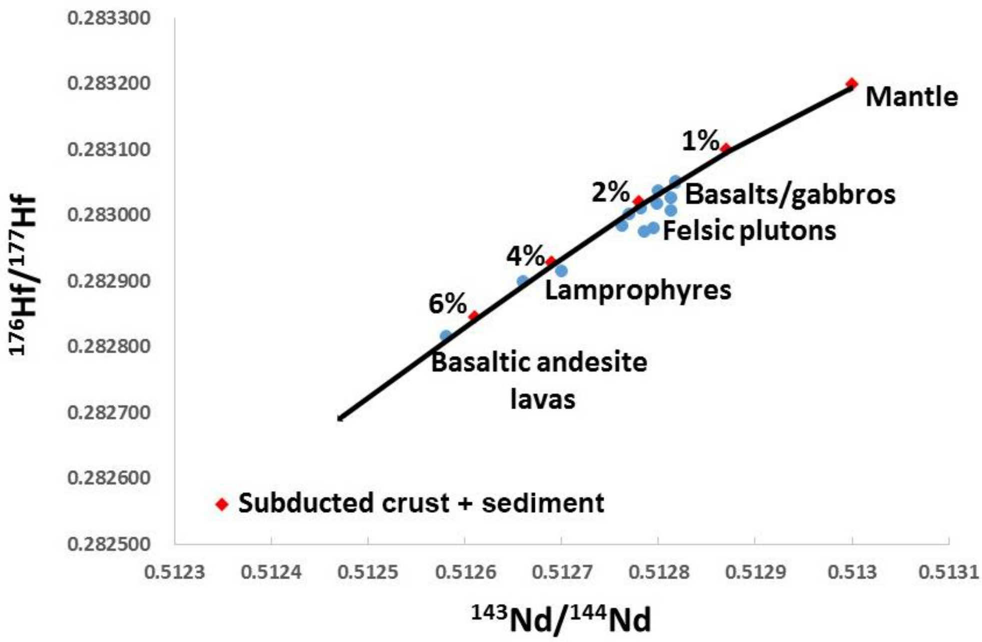

Figure 9. $^{176}Hf/^{177}Hf$ versus $^{143}Nd/^{144}Nd$ for samples from El Teniente (Table 2; blue circles) compared to isotopic values of a primitive mantle (Table 3) modified by the addition of various proportions (red diamonds) of subducted crust and sediment.

In summary, the Hf isotopic data are consistent with Sr, Nd and Pb isotopic data, and suggest the incorporation of small but progressively increasing proportions of continental crust in the mantle source of the mafic magmas erupted in the vicinity of El Teniente between 15 and 2.3 Ma. Trench sediment recycling has been confirmed by the detection of cosmogenic ^{10}Be in many, including Andean arc, lavas [59-61], and comprehensive trace-element and isotopic studies have also provided evidence for the incorporation of fore-arc eroded crust in the subarc mantle source of both Andean [3-5,7,8,10,11] and arc volcanoes along other convergent plate boundaries [58,62-64]. The model developed for the El Teniente area suggests that increasing rates of subduction erosion through time has resulted in variable, but nevertheless relatively small (1 to ≤6 %) amounts of subducted crust having significantly affecting the isotopic composition of the mantle source of the mafic magmas through time. Models for magmagenesis in other arcs, for instance the central Mexican volcanic belt, have suggested much larger amounts of recycled crust involved in the generation of both mafic and intermediate arc magmas; from >60% in conjunction with diapiric uprise and melting of subducted crust [58] to 100% resulting in the generation of andesites by bulk melting of subducted crust "relaminated" below the mantle wedge [63].

5.2. El Teniente deposit

The giant El Teniente Cu-Mo deposit originally contained ≥100 million metric tonnes (Mt) of Cu [32,33]. Pb, S and Os isotopic data [43-45,65] indicate that Cu, Mo and S were derived from the associated igneous rocks. O and H isotopic and fluid inclusion data suggest that these metals were

 doi:10.20944/preprints201907.0327.v1

transported and deposited by high-temperature magmatic fluids [38,39,66], and a significant proportion of the Cu ore is contained with magmatic-hydrothermal breccia pipes [32-36]. Important questions concerning the genesis of El Teniente, and any other giant orthomagmatic ore deposit, are: 1) Was the large amount of metal in the deposit derived from a large amount of magma or a unique metal-rich magma?; and 2) How were the metals transferred from the magma into the host rocks?

Muñoz et al. [37] conclude that the high initial ε_{Hf} values (total average of +7.4) of the syn-mineralization felsic plutons "rules out involvement of any significant crustal contamination in the genesis of the El Teniente magmas." We agree, at least with regard to intra-crustal assimilation (MASH). However, they then go on to suggest, based "entirely on the near constant Hf isotopic composition shown by the Cenozoic igneous of the region" that they also "envision that Cenozoic magmatism in central Chile originates from a MASH reservoir." We disagree, given the clear evidence that the ε_{Hf} values of Cenozoic magma, in particular mantle-derived mafic magmas erupted in the region, were not at all constant, but progressively decreased significantly with time.

We suggest instead that the near constancy of the Hf isotopic composition of the 7.1 to 4.8 Ma felsic plutons in the El Teniente deposit is a result of mixing, storage and homogenization (but not crustal assimilation) of mantle-derived magmas in a large vertically zoned upper crustal magma chamber (Figure 10) which developed as a result of compressive deformation after 7 Ma (Figure 8). These mafic mantle-derived magmas provided heat, water, S and metals into the base of this magma chamber [67], which became vertically stratified with more hydrous and more silica-rich magmas closer to the surface. As the input of mantle-derived magmas decreased during the Late Miocene, and uplift and erosion brought the roof of the chamber closer to the surface [12,13], the upper part of the chamber crystallized and differentiated into the magmas that formed the felsic plutons. Although the Hf isotopic composition of the mantle-derived magmas may have been evolving over this same time period (Figure 7), the large volume of the magma chamber into which these magmas mixed limited the variations observed within the progressively younger felsic plutons, although some decrease in their ε_{Hf} values is apparent. Once this large magma chamber fully crystallized, mantle-derived olivine lamprophyre dikes were able to penetrate up to the surface, and these clearly exhibit lower ε_{Hf} resulting from increased source region contamination of the mantle by subducted components.

Muñoz et al. [37] further suggest that, as a result of crustal thickening, dehydration melting in the deep crustal hot zone [68] within which the MASH reservoir was located "probably influenced the fertility of the magmas by increasing the melt component derived from this process relative to the component derived from primary" mantle melts. They do not detail what specific characteristics make a magma more "fertile", but they note that dehydration melting leads to the development of water undersaturated magmas, which are less, not more likely to be able to exsolve mineral-rich magmatic fluids.

In contrast, we do conclude that the mantle-derived olivine basalts emplaced in the Teniente Mafic Complex prior to the development of the large magms chamber below the deposit, and the mantle-derived olivine lamprophyres which cut through the deposit after this magma chamber fully solidified, have changed their isotopic compositions due to increased contamination of the mantle source region with subducted components, but we do not observe [22,23] any significant change in the Cu contents between the pre-mineralization olivine basalts (100 ppm) and the post-mineralization olivine lamprophyres (100 ppm). Therefore we do not believe that source region contamination

 doi:10.20944/preprints201907.0327.v1

generated a uniquely "fertile" magma with respect to Cu content. We have suggested instead that the large amount of Cu in the deposit reflects a large amount of magma in the chamber above which the deposit developed [38,39,69,70]. To produce the ≥100x10^6 tonnes of Cu in the deposit requires a batholith-size (≥600 km^3) amount of magma with ~100 ppm Cu. What made the deposit giant was that over the ~3 m.y. period that a magma chamber existed below the developing deposit, Cu, S heat and water from mantle derived magmas were added continuously to the base of the chamber and subsequently concentrated near the roof of the chamber by volatile transport. Clearly, because of increased source region contamination by subducted materials the mantle wedge did became progressively more hydrated, ultimately leading to the generation of lamprophyric magmas, which require 6-16 wt % H_2O, instead of olivine basalts, which require only 2 wt % H_2O [52-55]. Increasing H_2O content of the mantle-derived magmas through the time that they were mixed into the overlying magmas chamber may have resulted in more oxidizing conditions within the chamber, enhancing the process of volatile transfer of S and metals towards the roof of the chamber (Figure 10; [49,51,71].

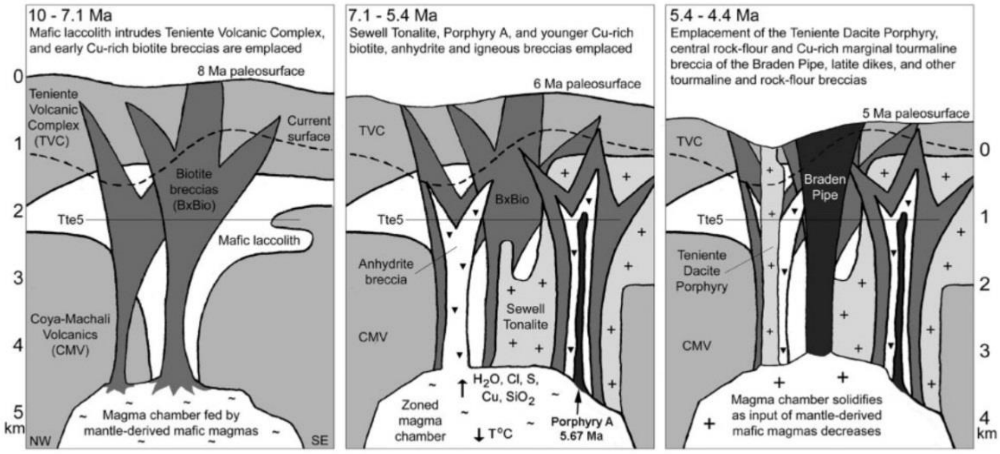

Figure 10. Model for the multistage development of the El Teniente deposit [23,32,33,39]. The main features of the model include (1) a large, long-lived (≥3 Myr) open-system magma chamber, crystallizing at ≥4 km depth, fed from below by mantle-derived mafic magmas and exsolving mineral-rich high-temperature magmatic fluids through its roof to produce the large breccia pipes that are prominent features this deposit; (2) decreasing magma supply in the Late Miocene and Pliocene as subduction angle decreases, leading to crystallization and solidification of this chamber; (3) progressive uplift and erosion that enhances this crystallization and solidification process and results in telescoping of different types of breccia and igneous rocks [12,13]; (4) progressive igneous differentiation of the magma chamber associated with crystallization and volatile loss, generating felsic porphyries that intrude previously mineralized rocks above the chamber. No coeval volcanism is known to have occurred during mineralization, but once the chamber solidified, post-mineralization mantle-derived olivine lamprophyre dikes were emplaced.

Older studies of El Teniente suggested that Cu was transferred into the host rocks in association with the intrusion of the Teniente Dacite Porphyry, but new age dates indicate that much of the mineralization preceds this event, and that this essentially barren porphyry, where it intrudes outside the deposit, creates alteration but not mineralization. Instead we have suggested that the Cu and S were transferred into the host rocks of the deposit from the roof of the large magma chamber by exsolution of high-temperature metal-rich fluids generating multiple large magmatic-hydrothermal mineralized breccia complexes such as the central Braden Pipe, and El Teniente is thus better classified as a megabreccia deposit (Figure 10; [23,32,33,38,39]. Vry et al. [36] suggested that such breccias formed in association with the intrusion of the small dacite and diorite dikes to the northeast of the Braden pipe (Figure 6). However, we suggest instead that the breccias formed first and the porphyries intruded into the zone of weakness created by the breccias, since some of these porphyry bodies, such as Porphyry A (Figure 6) contain clasts of the breccias they intrude, and others of these small porphyries have no associated breccias surrounding them.

6. Conclusions

1. The Hf isotopic data are consistent with the Sr, Nd and Pb data, and imply the incorporation of small, but progressively increasing proportions of continental crust into the mantle source of the mafic magams erupted in the vicinity of El Teniente between ≥15 and 2.3 Ma.
2. The felsic plutons in the deposit formed by mixing, storage and homogenization, combined with crystal-liquid differentiation, but not crustal assimilation (not MASH), in a large, long-lived, vertically zoned magma chamber that developed due to compressive deformation and persisted between the period ~7 to 4.6 Ma.
3. Progessively more hydrous and radiogeneic mantle-derived mafic magmas feed this chamber from below, providing heat, H_2O, S and metals, but no unique "fertile" Cu-rich magma was involved in the formation of the deposit.
4. As the volume of these mantle-derived magmas decreased from the Late Miocene into the Pliocene, the chamber crystallized and solidified, producing both felsic plutons and large magmatic-hyrothermal breccias that emplaced Cu and S into the older (≥8.9 Ma) mafic Teniente Mafic Complex host rocks of the deposit. The deposit is therefore best classified as a megabreccia deposit.

Author Contributions: Conceptualization, Charles R Stern, M Alexandra Skewes and Alejandra Arévalo; Data curation, Kwan-Nang Pang and Hao-Yang Lee; Project administration, Charles R Stern, M Alexandra Skewes and Alejandra Arévalo; Writing – original draft, Charles R Stern; Writing – review & editing, Kwan-Nang Pang, Hao-Yang Lee, M Alexandra Skewes and Alejandra Arévalo.

Funding: The analytical work was supported by Ministry of Science and Technology, Republic of China (Taiwan) grant MOST 105-2628-M-001-002-MY4 to K.-N.P.

Acknowledgments: We thank Patricio Zuñiga, Ricardo Floody, Domingo Espiñeira and René Padilla for collaboration in the collection and characterization of the samples from El Teniente.

Conflicts of Interest: We have no conflicts of interests.

References

1. Hickey-Vargas, R. Peeled or MASHed? *Nature* **1991**, *350*, 381-382.
2. Hildreth, W.; Moorbath, S. Crustal contributions to arc magmatism in the Andes of central Chile. *Contrib. Mineral. Petrol.* **1988**, *103*, 361-386.
3. Stern, C.R. Role of subduction erosion in the generation of Andean magmas. *Geology* **1991**, *19*, 78-81.
4. Stern, C.R. Active Andean volcanism: its geologic and tectonic setting. *Rev. Geol. Chile* **2004**, *31*, 161-208.

5. Stern, C.R. Subduction erosion: rates, mechanisms, and its role in arc magmatism and the evolution of the continental crust and mantle. *Gondwana Res.* **2011**, *20*, 284–308.
6. Rutland, R.W.R. Andean orogeny and ocean floor spreading. *Nature* **1971**, *233*, 252-255.
7. Goss, A.R.; Mahlburg Kay, S.; Mpodozis, C. Andean adakite-like high-Mg andesites on the Northern margin of the Chilean-Pampean flat-slab (27–28.5°S) associated with frontal arc migration and fore-arc subduction erosion. *J. Petrol*. **2013**, *54*, 2193–2234.
8. Risse, A.; Trumbull, R.B.; Kay, S.M.; Coira, B.; Romer, R.L. Multi-stage evolution of Late Neogene mantle-derived Magmas from the Central Andes Back-arc in the Southern Puna Plateau of Argentina. *J. Petrol.* **2013**, *10*, 1963–1995.
9. Lamb. S.; Davis, P. Cenozoic climate change as a possible cause for the rise of the Andes. *Nature* **2003**, *425*, 792-797.
10. Kay, S.M.; Godoy, E.; Kurtz, A. Episodic arc migration, crustal thickening, subduction erosion, and magmatism in the south-central Andes. *Geol. Soc. Amer. Bull.* **2005**, *117*, 67-88.
11. Holm, P.M.; Søager, N.; Thorup-Dyhr, C.; Rohde-Nielsen, M. Enrichments of the mantle sources beneath the Southern Volcanic Zone (Andes) by fluids and melts derived from abraded upper continental crust. *Contrib. Mineral. Petrol.* **2014**, *167*, 1004.
12. Skewes, M.A.; Holmgren, C. Solevantamiento Andino, erosión y emplazamiento de brechas mineralizadas en el depósito de cobre porfídico Los Bronces, Chile Central (33°S): aplicación de termometría de inclusiones fluidas. *Rev. Geol. Chile* **1993**, *20*, 71-84.
13. Skewes, M.A.; Stern, C.R. Tectonic trigger for the formation of late Miocene Cu-rich breccia pipes in the Andes of central Chile. *Geology* **1994**, *22*, 551-554.
14. Kurtz, A.C.; Kay, S.M.; Charrier, R.; Farrar, E. Geochronology of Miocene plutons and exhumation history of the El Teniente region, Central Chile (34-35°S). *Rev. Geol. Chile* **1997**, *16*, 145-162.
15. Charrier, R.; Baeza, O.; Elgueta, S.; Flynn, J.J.; Gans, P.; Kay, S.M.; Muñoz, N.; Wyss, A.R.; Zurita, E. Evidence for Cenozoic extensional basin development and tectonic inversion south of the flat-slab segment, southern Central Andes, Chile (33°-36°S.L.). *J. S. Amer. Earth Sci.* **2002**, *15*, 117-139.
16. Giambiagi, L.B.; Ramos, V.A. Structural evolution of the Andes in a transitional zone between flat and normal subduction (33°30-33°45'S), Argentina and Chile. *J. S. Amer. Earth Sci.* **2002**, *15*, 101-116.
17. Nyström, J.; Vergara, M.; Morata, D.; Levi, B. Tertiary volcanism during extension in the Andean foothills of central Chile (33°15'-33°45'S). *Geol. Soc. Amer. Bull.* **2003**, *115*, 1523-1537.
18. Farías, M.; Charrier, R.; Carretier, S.; Martinod, J.; Fock, A.; Campbell, D.; Cáceres, J.; Comte, D. Late Miocene high and rapid surface uplift and its erosional response in the Ande of central Chile (33º-35ºS). *Tectonics* **2008**, *27*, TC1005.
19. Farías, M.; Comte, D.; Charrier, R.; Martinod, J.; Tassara, A.; Fock, A. Crustal-scale structural architecture of the central Chile Andes based on 3D seismic tomography, seismicity, and surface geology: implications for mountain building in subduction zones. *Tectonics* **2010**, *29*, TC3006.
20. Giambiagi, L.B.; Mescua, J.; Bechis, F.; Tassara, A.; Hoke, G. Thrust belts of the southern Central Andes: Along-strike variations in shortening, topography, crustal geometry, and denudation: *Geol. Soc. Amer. Bull.* **2012**, *124*, 1339–1351.
21. Stern, C.R.; Skewes, M.A. Miocene to present magmatic evolution at the northern end of the Andean Southern Volcanic Zone, central Chile. *Rev. Geol. Chile* **1995**, *22*, 261-272.
22. Stern, C.R.; Floody, R.; Espiñeira, D. Pliocene olivine-hornblende-lamprophyre dikes from Quebrada de los Sapos, El Teniente, Central Chile (34°S): Implications for the subarc mantle. *Andean Geol.* **2011**, *38*, 1-22.

 doi:10.20944/preprints201907.0327.v1

23. Stern, C.R.; Skewes, M.A.; Arévalo, A. Magmatic evolution of the giant El Teniente Cu-Mo deposit, Central Chile. *J. Petrol.* **2012**, *52*, 1591-1617.
24. Muñoz, M.; Farías, M.; Charrier, R.; Fanning, C.M.; Polvé, M.; Deckart, K. Isotopic shifts in the Cenozoic Andean arc of central Chile: records of an evolving basement throughout cordilleran arc mountain building. *Geology* **2013**, *41*, 931-934.
25. Stern, C.R. Pliocene to present migration of the volcanic front, Andean Southern Volcanic Zone. *Rev. Geol. Chile* **1989**, *16*, 145-162.
26. Yáñez, G.; Ranero, C.; von Huene, R.; Díaz, J. Magnetic anomaly interpretation across the southern Central Andes (32°-33.5°S): the role of the Juan Fernández ridge in the late Tertiary evolution of the margin. *J. Geophys. Res.* **2001**, *106*, 6325-6345.
27. Yáñez, G.; Cembrano, J.; Pardo, M.; Ranero, C.; Selles, D. The Challenger-Juan Fernández-Maipo major tectonic transition of the Nazca-Andean subduction system at 33-34°S: geodynamic evidence and implications. *J. S. Amer. Earth Sci.* **2002**, *15*, 23-38.
28. Lindgren, W.; Bastin, E.S. Geology of the Braden mine, Rancagua, Chile. *Econ. Geol.* **1922**, *17*, 75-99.
29. Howell, F.H.; Molloy, S. Geology of the Braden orebody, Chile, South America. *Econ. Geol.* **1960**, *70*, 863-905.
30. Camus, F. Geology of the El Teniente orebody with emphasis on wall-rock alteration. *Econ. Geol.* **1975**, *70*, 1341-1372.
31. Cuadra, P. Geocronología K-Ar del yacimiento El Teniente y áreas adyacentes. *Rev. Geol. Chile* **1986**, *27*, 3-26.
32. Skewes, M.A.; Arévalo, A., Floody, R., Zuñiga, P.; Stern, C.R. The giant El Teniente breccia deposit: hypogene copper distribution and emplacement. In *Global Exploration 2002: Integrated Methods of Discovery*, Goldfarb, R.J., Nielson, R.L. Eds.; Society of Economic Geologists: USA, 2002; Special Publications 9, pp. 299-332.
33. Skewes, M.A.; Arévalo, A.; Floody, R.; Zuñiga, P.; Stern, C.R. The El Teniente megabreccia deposit, the world's largest copper deposit. In *Super Porphyry Copper and Gold Deposits: A Global Perspective*, Porter, T.M., Ed.; PGC Publishing: Adelaide, Australia, 2005; Volume 1, pp. 83-114.
34. Maksaev, V.; Munizaga, F.; McWilliams, M.; Fanning, M.; Marther, R.; Ruiz, J.; Zentilli, M. Chronology for El Teniente, Chilean Andes, from U-Pb, $^{40}Ar/^{39}Ar$, Re-Os, and fission track dating: implications for the formation of a supergiant porphyry Cu-Mo deposit. In *Andean Metallogeny: New Discoveries, Concepts and Updates*, Sillitoe, R.H., Perelló, J., Vidal, C.E. Eds.; Society of Economic Geologists: USA, 2004; Special Publications 11, pp. 15-54.
35. Cannell, J.; Cooke, D.; Walshe, J.L.; Stein, H. Geology, mineralization, alteration, and structural evolution of El Teniente porphyry Cu-Mo deposit. *Econ. Geol.* **2005**, *100*, 979-1004.
36. Vry, V.H.; Wilkinson, J.J.; Seguel, J.; Millán, J. Multistage intrusion brecciation and veining at El Teniente, Chile: evolution of a nested porphyry system. *Econ. Geol.* **2010**, *105*, 119-153.
37. Muñoz, M.; Charrier, R.; Fanning, C.M.; Maksaev, V.; and Deckart, K. Zircon trace element and O-Hf isotope analyses of mineralized intrusions from El Teniente ore deposit, Chilean Andes: Constraints on the source and magmatic evolution of porphyry Cu-Mo related magmas. *J. Petrol.* **2012**, 53, 1091–1122.
38. Skewes, M.A.; Stern, C.R. Genesis of the giant Late Miocene to Pliocene copper deposits of central Chile in the context of Andean magmatic and tectonic evolution. *Internat. Geol. Rev.* **1995**, *37*, 71-84.
39. Stern, C.R.; Skewes, M.A. Origin of giant Miocene and Pliocene Cu-Mo deposits in Central Chile: Role of ridge subduction, decreased subduction angle, subduction erosion, crustal thickening and long-lived,

batholiths-size, open system magma chambers. In *Super Porphyry Copper and Gold Deposits: A Global Perspective,* Porter, T.M., Ed.; PGC Publishing: Adelaide, Australia, 2005; Volume 1, pp. 65-82.
40. Warnaars, F.W.; Holmgren, C; Barassi, S. Porphyry copper and Tourmaline breccias at Los Bronces-Río Blanco, Chile. *Econ. Geol.* **1985**, *80*, 1544-1565.
41. Skewes, M.A.; Stern, C.R. Late Miocene mineralized breccias in the Andes of central Chile: Sr- and Nd-isotopic evidence for multiple magmatic sources. In Andean Copper Deposits, Camus, F., Sillitoe, R.H., Petersen, R., Eds.; Society of Economic Geologists: USA, 1996; Special Publications 5, pp. 119-130.
42. Skewes, M.A.; Holmgren, C.; Stern, C.R. The Donoso copper-rich, tourmaline-bearing breccia pipe in central Chile: petrologic, fluid inclusion and stable isotope evidence for an origin from magmatic fluids. *Mineral. Deposita* **2003**, *38*, 2-21.
43. Kusakabe, M.; Hori, M.; Nakagawa, S.; Matsuhisa, Y.; Ojeda, J.M.; Serrano, L.M. Oxygen and sulfur isotopic compositions of quartz, anhydrite and sulfide minerals from the El Teniente and Río Blanco porphyry copper deposits, Chile. *Bull. Geol. Survey Japan* **1984**, *35*, 583-614.
44. Kusakabe, M., Hori, M. & Matsuhisa, Y. Primary mineralization-alteration of the El Teniente and Río Blanco porphyry copper deposits, Chile; stable isotope, fluid inclusion and Mg+2/Fe+2/Fe+3 ratios of hydrothermal fluids. In *Stable Isotopes and Fluid Processes in Mineralization*, Herbert, H.K., Ho, S.E., Eds.; University of Western Australia Press, Perth, Australia, 1990; pp. 244-259.
45. Puig, A. Geologic and metallogenic significance of the isotopic composition of lead in galenas of the Chilean Andes. *Econ. Geol.* **1988**, *83*, 843-858.
46. Muñoz, M.; Fuentes, F.; Vergara, M.; Aguirre, L.; Nyström, J.O. Abanico East Formation: petrology and geochemistry of volcanic rocks behind the Cenozoic arc front in the Andean Cordillera, central Chile (33°50'S). *Rev. Geol. Chile* **2006**, *33*, 109-140.
47. Montecinos, P.; Schárer, U.; Vergara, M.; Aguirre, L. Lithospheric origin of Oligocene--Miocene magmatism in Central Chile: U-Pb ages and Sr-Pb-Hf isotope composition of minerals. *J. Petrol*. **2008**, *49*, 555-580.
48. Godoy, E.; Yáñez, G.; Vera, E. Inversion of an Oligocene volcanic^ tectonic basin and uplifting of its superimposed Miocene magmatic arc in the Chilean Central Andes: first seismic and gravity evidences. *Tectonophys.* **1999**, *306*, 217-236.
49. Stern, C.R.; Funk, J.A.; Skewes, M.A.; Arévalo, A. Magmatic anhydrite in plutonic rocks at the El Teniente C^Mo deposit, Chile, and the role of sulfur- and copper-rich magmas in its formation. *Econ. Geol.* **2007**, *102*, 1335-1344.
50. Deckart, K.; Godoy, E.; Bertens, A.; Saeed, A.; Jeréz, D. Barren Miocene granitoids in the central Andean metallogenic belt, Chile: Geochemistry and Nd-Hf and U-Pb isotope systematics: *Andean Geol.* **2010**, *37*, 1–31.
51. Blatter, D.K.; Carmichael, I.S.E. Hornblende peridotite xenoliths from central Mexico reveal the highly oxidized nature of subarc upper mantle. *Geology* **1998**, *26*, 1035-1038.
52. Blatter, D.K.; Carmichael, I.S.E. Hydrous phase equilibria of a Mexican high-silica andesite: a candidate for mantle origin? *Geochim. Cosmochim. Acta* **2001**, *65*, 4043-4065.
53. Moore, G.M.; Carmichael, I.S.E. The hydrous phase equilibra (to 3kbar) of an andesite and basaltic andesite from Western Mexico: constraints on water content and conditions of phenocrysts growth. *Contrib. Mineral. Petrol.* **1998**, *130*, 304-319.
54. Carmichael, I.S.E. The andesite aqueduct: perspectives in the evolution of intermediate magmas in west-central Mexico. *Contrib. Mineral. Petrol.* **2002**, *143*, 641-663.

 doi:10.20944/preprints201907.0327.v1

55. Barcley, J.; Carmichael, I.S.E. A Hornblende Basalt from Western Mexico: Water-saturated Phase Relations Constrain a Pressure-Temperature Window of Eruptibility. *J. Petrol.* **2004**, *45*, 485-506.
56. Rudnick R.; Gao S. Composition of the continental crust. In *The Crust*, R. L. Rudnick, R.L., Ed.; Elsevier-Pergamon, Oxford, Englanf, 2002; pp. 1–64.
57. McDonough W.F.; Sun S.S. The composition of the Earth. *Chem. Geol.***1995**, *120*, 223–253.
58. Straub, S.M.; Gómez-Tuena, A.; Bindeman, I.N.; Bolge, L.L.; Brandl, P.A.; Espinasa-Perena, R.; Solari, L.; Stuart, F.M.; Vannucchi, P.; Zellmer, G.F. Crustal recycling by subduction erosion in the central Mexican Volcanic Belt. *Geochim. Cosmochim. Acta* **2015**, *166*, 29–52.
59. Tera F.; Brown L.; Morris J.; Sacks I.S. Sediment incorporation in island-arc magmas: Inferences from ^{10}Be. *Geochim. Cosmochim. Acta* **1986**, *50*, 535–550.
60. Morris J.D.; Leeman W.P.; Tera F. The subducted component in island arc lavas: constraints from Be isotopes and B–Be systematics. *Nature* **1990**, *344*, 31–36.
61. Morris J.D.; Gosse J.; Brachfeld, S.; Tera F. Cosmogenic ^{10}Be and the solid earth: studies in geomagnetism, subduction zone processes, and active tectonics. In *Reviews in Mineralogy*, Grew, E., Ed.; Mineralogical Society of America, Washington, DC, USA, 2002; pp. 207–270.
62. Tonarini S.; Leeman W.P.; Leat P.T. Subduction erosion of forearc mantle wedge implicated in the genesis of the South Sandwich Island (SSI) arc: evidence from boron isotope systematics. *Earth Planet. Sci. Lett.* **2011**, *301*, 275–284.
63. Gómez-Tuena, A.; Cavazos-Tovar, J.G.; Parolari, M.; Straub, S.M.; Espinasa-Pereña, R. Geochronological and geochemical evidence of continental crust 'relamination' in the origin of intermediate arc magmas. *Lithos* **2018**, *322*, 52-66.
64. Goss, A.R.; Kay, S.M. Steep REE patterns and enriched Pb isotopes in southern Central American arc magmas: evidence for forearc subduction erosion? *Geochem. Geophys. Geosyst.* **2006**, *7*, 1-20.
65. Freydier, C.; Ruiz, J.; Chesley, J.; Candless, T.; Munizaga, F. Re-Os isotope systematics of sulfides from felsic igneous rocks: application to base metal porphyry mineralization in Chile. *Geology* **1997**, *25*, 775-778.
66. Klemm, L.M.; Pettke, T.; Heinrich, C.L.; Campos, E. Hydrothermal evolution of the El Teniente deposit, Chile: porphyry Cu-Mo ore deposition from low-salinity magmatic fluids. *Econ. Geol.* **2007**, *102*, 1021-1045.
67. Hattori, K.H.; Keith, J.D. Contributions of mafia melt for porphyry deposits: evidence from Pinatubo and Bingham. *Mineral. Deposita* **2001**, *36*, 799-806.
68. Annen, C.; Blundy, J.D.; Sparks, R.S.J. The genesis of intermediate and silica magmas in deep crustal hot zones. *J. Petrol.* **2006**, *47*, 505-539.
69. Cloos, M. Bubbling magma chambers, cupulas and porphyry copper deposits. *Internat. Geol. Revs.* **2001**, *43*, 285-311.
70. Richards, J.P. Cumulative factors in the generation of giant calc-alkaline porphyry Cu deposits. In *Super Porphyry Copper and Gold Deposits: A Global Perspective*, Porter, T.M., Ed.; PGC Publishing, Adelaide, Australia, 2005; Volume 1, pp. 7-26.
71. Garrido, I.; Cembrano, J.; Siña, A.; Stedman, P.; Yáñez, G.A. High magma oxidation state and bulk crustal shortening: key factors in the genesis of Andean porphyry copper deposits, central Chile (31-34°S). *Rev. Geol. Chile* **2002**, *29*, 43-54.